

1 An Artificial Neural-Network Approach for Motor

2 Hotspot Identification Based on Electroencephalography:

3 A Proof-of-Concept Study

4
5 Ga-Young Choi¹, Chang-Hee Han², Hyung-Tak Lee¹, Nam-Jong Paik³, Won-Seok Kim³,
6 Han-Jeong Hwang^{1,*}

7 E-mail: cgy326@naver.com, zeros8706@naver.com, falling_slow@naver.com, njpaik@snu.ac.kr,
8 wondol77@gmail.com, hwanghj@korea.ac.kr

9
10 ¹Department of Electronics and Information Engineering, Korea University, Sejong 30019,
11 Republic of Korea

12 ²Machine Learning Group, Berlin Institute of Technology (TU Berlin), Berlin 10623,
13 Germany

14 ³Department of Rehabilitation Medicine, Seoul National University College of Medicine,
15 Seoul National University Bundang Hospital, Seongnam-si 13620, Republic of Korea

16 *Corresponding Authors
17
18

19 **Corresponding Author Information:**

20 **Name:** Won-Seok Kim

21 **Address:** Department of Rehabilitation Medicine, Seoul National University College of
22 Medicine, Seoul National University Bundang Hospital, Seongnam-si 13620, Republic of
23 Korea

24 **E-mail:** wondol77@gmail.com

25
26 **Name:** Han-Jeong Hwang

27 **Address:** Department of Electronics and Information Engineering, Korea University, Sejong
28 30019, Republic of Korea

29 **E-mail:** hwanghj@korea.ac.kr

Abstract

30
31
32
33
34
35
36
37
38
39
40
41
42
43
44
45
46
47
48
49
50
51
52
53
54
55
56
57

Background: To apply transcranial electrical stimulation (tES) to the motor cortex, motor hotspots are generally identified using motor evoked potentials by transcranial magnetic stimulation (TMS). The objective of this study is to validate the feasibility of a novel electroencephalography (EEG)-based motor-hotspot-identification approach using a machine learning technique as a potential alternative to TMS.

Methods: EEG data were measured using 63 channels from thirty subjects as they performed a simple finger tapping task. Power spectral densities of the EEG data were extracted from six frequency bands (delta, theta, alpha, beta, gamma, and full) and were independently used to train and test an artificial neural network for motor hotspot identification. The 3D coordinate information of individual motor hotspots identified by TMS were quantitatively compared with those estimated by our EEG-based motor-hotspot-identification approach to assess its feasibility.

Results: The minimum mean error distance between the motor hotspot locations identified by TMS and our proposed motor-hotspot-identification approach was 0.22 ± 0.03 cm, demonstrating the proof-of-concept of our proposed EEG-based approach. A mean error distance of 1.32 ± 0.15 cm was measured when using only nine channels attached to the middle of the motor cortex, showing the possibility of practically using the proposed motor-hotspot-identification approach based on a relatively small number of EEG channels.

Conclusion: We demonstrated the feasibility of our novel EEG-based motor-hotspot-identification method. It is expected that our approach can be used as an alternative to TMS for motor hotspot identification. In particular, its usability would significantly increase when using a recently developed portable tES device integrated with an EEG device.

Keywords –Motor hotspot; Electroencephalography; Transcranial electrical stimulation; Machine learning; Artificial neural-network

58 **Introduction**

59 Motor impairment is a frequent symptom occurring after neurological disorders, such as
60 stroke and Parkinson's disease [1–3]. Although motor functions are not completely restored
61 after neurological disorders, continuous rehabilitation is necessary to prevent muscle loss and
62 the retrogression of intact motor functions. Conventional motor rehabilitation interventions
63 involve specific movements related to the affected limbs, which are enforced by a therapist or
64 an assistive rehabilitation device.

65 Recently, transcranial electrical stimulation (tES) capable of modulating cortical excitability
66 using a weak electrical current has been introduced for motor rehabilitation, and its positive
67 effects have been proven in many interventional studies even though the mechanisms have not
68 yet been fully understood [4–10]. For example, one study showed that anodal transcranial direct
69 current stimulation (tDCS) on the ipsilesional primary motor cortex could improve overall
70 motor functions of the upper limbs in stroke patients, and its effects persisted for at least 3
71 months post-intervention [11]. Another study also demonstrated the positive effects of
72 transcranial alternating current stimulation (tACS) on motor performance improvements in
73 Parkinson's disease [12].

74 To maximize the positive effects of tES on motor rehabilitation, it is important to find an
75 optimal tES target location. The lesional primary motor area (M1) and its contralateral motor
76 area have been traditionally used as stimulation target locations, to which anodal and cathodal
77 tES electrodes are applied, respectively [13–15]. A cathodal tES electrode is sometimes applied
78 to the contralateral supraorbital area of the lesional hemisphere instead of the contralateral
79 motor area, called the M1-supraorbital prominence [15–17]. Identifying M1 can be performed
80 by either the international 10-20 coordinate system used for electroencephalography (EEG)
81 measurements or motor evoked potentials (MEPs), induced by transcranial magnetic

82 stimulation (TMS). The former method uses C3 on the left hemisphere or C4 on the right
83 hemisphere as the M1 location, depending on the lesional side [13, 18]. However, as the
84 international 10-20 coordinate system does not consider inter-subject variability in cortical
85 anatomy, the M1 location (C3 or C4) found by the international 10-20 coordinate system might
86 not be an appropriate tES target location for motor rehabilitation. In particular, patients with
87 neurological disorders, who are the main recipients of tES treatment, have shown significant
88 changes in cortical morphologies owing to neural reorganization and plasticity after the
89 occurrence of neurological diseases, such as stroke and cerebral palsy [19], requiring better
90 methods to find individualized tES target locations more precisely.

91 As an alternative to the international 10-20 coordinate system, many studies have used TMS-
92 induced MEP to find an individualized tES target location, called motor hotspot, for motor
93 rehabilitation. This has been done because applying tES to the motor hotspot found by TMS-
94 induced MEP could provide focal and accurate neuromodulatory effects on the motor network
95 [20–22]. TMS is a useful tool to find motor hotspots, but requires a relatively bulky device and
96 a somewhat cumbersome procedure accompanying the empirical judgment of a technician.
97 Moreover, another device that measures MEP is required to find an individual motor hotspot
98 using TMS.

99 In this study, we propose a novel alternative to TMS for motor hotspot identification based
100 on EEGs measured during a simple finger-tapping motor task. A machine learning technique
101 based on an artificial neural network (ANN) was applied to the measured EEG to localize
102 individualized motor hotspots. The motor hotspot positions estimated by our proposed EEG-
103 based machine-learning approach were then compared to those found by the traditional TMS-
104 induced MEP to verify the feasibility of our approach. Preliminary results have been shown in
105 [23].

106 **Methods**

107 **Subjects**

108 Thirty healthy subjects (10 females and 20 males; 25 ± 1.39 years; all right-handed)
109 participated in this study, and they had no history of psychiatric diseases that might affect
110 research results. All subjects received the information about the details of the experimental
111 procedure and signed an informed consent for participation in the study. Appropriate monetary
112 compensation for their participation was provided after the experiment. This study was
113 approved by the Institutional Review Board (IRB) of Kumoh National Institute of Technology
114 (No. 6250) and was conducted in accordance with the principles of the declaration of Helsinki.

115 **Motor Hotspot Identification by TMS-Induced MEP**

116 Before measuring the EEGs, the motor hotspots of both hands were identified for each
117 subject using the MEPs of the first dorsal interosseous (FDI) muscle. To this end, Ag-AgCl
118 disposable electrodes were attached to the FDI muscles of both hands to measure the MEPs
119 (actiCHamp, Brain Products GmbH, Gilching, Germany). We applied single-pulse TMS to the
120 contralateral motor cortex during the resting state (REMED., Daejeon, Korea), and determined
121 the motor hotspot location that showed the maximum MEP with individual minimum
122 stimulation intensity [24–26]. The motor hotspot locations were marked in a 3D coordinate
123 system based on the vertex (Cz in the international 10-20 system) using a 3D digitizer
124 (Polhemus Inc., Colchester, Vermont, USA), and they were used as the ground truth to compare
125 with those estimated by our EEG-based motor-hotspot-identification approach.

126 **EEG Recording**

127 After identifying the individual motor hotspots using TMS for both hands, task-related EEG

128 data were measured using 63 EEG electrodes attached to the scalp based on the international
129 10-20 system (Figure 1). The ground and reference electrodes were attached to Fpz and FCz,
130 respectively. The positions of the EEG electrodes were marked in the 3D coordinate system as
131 for the motor hotspot locations identified by TMS-induced MEPs. The EEG data were sampled
132 at 1,000 Hz using a multi-channel EEG acquisition system (actiCHamp, Brain Products GmbH,
133 Gilching, Germany) while the subjects were performing a simple finger-tapping motor task.
134 Each subject performed the task 30 times, which consisted of pressing a button using their
135 index fingers whenever a red circle was presented in the center of a monitor (Figure 2); two
136 EEG measurement sessions were independently conducted using the left and right index fingers,
137 respectively. The subjects were given sufficient rest whenever they wanted during the
138 experiment to avoid fatigue. Moreover, they were instructed to remain relaxed during the
139 experiment without any movement to prevent unwanted physiological artifacts. Because we
140 carried out preliminary experiments with the first two subjects to validate our experimental
141 paradigm before the main experiment, the right hand was only employed for these two subjects.
142 In addition, we excluded the EEG data of one subject for both hands, and those of the left hand
143 for other three subjects due to high contamination of EEG data caused by physiological artifacts.
144 Thus, 29 and 25 EEG datasets were used for the right and left hands, respectively, for data
145 analysis.

146 **EEG-Based Motor Hotspot Identification**

147 EEG signal preprocessing was performed using the EEGLAB toolbox based on MATLAB
148 2017b (MathWorks, Natick, MA, USA). The raw EEG data were first down-sampled into 200
149 Hz to which we sequentially applied common average reference and bandpass filtering between
150 0.5 and 50.5 Hz (zero-phase 3rd-order Butterworth filter). Independent component analysis
151 (ICA) was then applied to the filtered EEG data to remove physiological artifacts. As

152 mentioned above, from visual inspection we excluded the EEG data significantly contaminated,
153 even after ICA application.

154 After preprocessing, we epoched EEG data between -0.5 and 0.5 s based on the key press
155 point for each trial to extract motor-related EEG features. Power spectral densities (PSDs) of
156 each EEG epoch were estimated in six frequency bands (delta: 1–4 Hz, theta: 4–8 Hz, alpha:
157 8–13 Hz, beta: 13–30 Hz, gamma: 30–50 Hz, and full: 1–50 Hz) using the fast Fourier
158 transform (FFT). An ANN was used to estimate the motor hotspot location using PSD features
159 where a subject-wise 10-fold cross-validation was performed with early stopping to prevent
160 overfitting. The PSD features of each channel and the 3D location coordinates of the motor
161 hotspot identified by TMS-induced MEP (ground truth) were used as the input for the ANN,
162 and the 3D location coordinates estimated using the PSD features were used as the output. The
163 numbers of input nodes, hidden nodes, and output nodes were 66 (63 channels + 3D motor
164 hotspot coordinate), 40 (empirically selected), and 3 (3D coordinate estimated by ANN),
165 respectively. We calculated the Euclidean distance between the 3D motor hotspot coordinates
166 identified by TMS and EEG to quantitatively estimate the error distance of our EEG-based
167 motor-hotspot-identification approach. The data analysis was independently performed for
168 each of the six EEG frequency bands.

169 To investigate the impact of the number of channels on the error distance, we repeatedly
170 performed the mentioned analysis by reducing the number of channels, in particular focusing
171 on the channels attached to the motor area (Figure 1). For this investigation, only gamma-band
172 PSD features (30–50 Hz) were used because they showed the best mean error distance when
173 using all 63 channels.

174

175 **Results**

176 Figure 3 shows the grand-average movement-related cortical potential (MRCP) measured
177 during finger tapping between -0.5 to 0.5 s based on the task onset, which was obtained by
178 averaging the MRCPs of four channels located on each hemisphere of the motor cortex to
179 confirm the reliability of our EEG data (baseline period: -1 to -0.5 s). MRCP was clearly
180 observed on the motor cortex during finger tapping for both hands, and, in particular, stronger
181 MRCP was observed on the contralateral motor area [27–28].

182 Figure 4(a) shows the mean error distances of the motor hotspot locations estimated by our
183 EEG-based machine learning approach for each hand with respect to the frequency band when
184 using all 63 channels. The PSD features of the relatively high frequency bands (beta, gamma,
185 and full bands) resulted in significantly lower mean error distances than those of the low
186 frequency bands (delta, theta, and alpha) for both hands (RM-ANOVA with Bonferroni
187 corrected p -value < 0.05 : delta = theta = alpha $>$ beta = gamma = full). No significant difference
188 was observed between the left and right hand for all the frequency bands in terms of the error
189 distance (paired t-test $p > 0.05$), except for the full band (right hand $>$ left hand). Figure 4(b)
190 shows a representative example of a single subject displaying the 3D locations of the motor
191 hotspot identified by TMS (blue rectangle) and those of our EEG-based approach for both
192 hands with respect to the frequency band. The motor hotspots estimated using the relatively
193 high frequency bands were found closer to the ground truth motor hotspot identified by TMS,
194 as compared to those estimated using the low frequency bands.

195 Figure 5(a) presents the mean error distances of the motor hotspot locations estimated by our
196 EEG-based approach for each hand with respect to the number of channels. In general, the
197 mean error distance monotonically and significantly increased as the number of channels

198 decreased (RM-ANOVA with Bonferroni corrected p -value < 0.05 : Ch_Set5 > Ch_Set4 >
199 Ch_Set3 = Ch_Set2 > Ch_Set1 for the right hand and Ch_Set5 > Ch_Set4 = Ch_Set3 > Ch_Set2
200 > Ch_Set1 for the left hand). No significant difference was observed between the left and right
201 hand for all channel sets in terms of the error distance (paired t-test $p > 0.05$), except Ch_Set3
202 (left hand > right hand). Figure 5(b) shows the 3D locations of the motor hotspots identified by
203 TMS and our EEG-based approach with respect to the number of channels, showing a similar
204 trend to the result shown in Figure 5(a).

205

206 Discussion

207 In this study, we proposed a novel EEG-based motor-hotspot-identification method using an
208 ANN as a potential alternative to TMS to determine a tES target location for motor
209 rehabilitation. A minimum mean error distance of 0.22 ± 0.03 cm was attained when using the
210 gamma band PSD information extracted using all 63 channels, demonstrating the proof-of-
211 concept of the proposed EEG-based motor-hotspot-identification method. An EEG device is
212 required for the use of the proposed motor-hotspot-identification approach based on a machine
213 learning technique. In recent years, a portable tES device integrated with an EEG device was
214 introduced (e.g., NeuroElectronics Starstim), which could facilitate the use of our motor-
215 hotspot-identification approach without using TMS.

216 To check the practical feasibility of the proposed motor-hotspot-identification method, the
217 effect of the number of channels was investigated using the gamma band PSD features. As
218 expected, the lowest mean error was obtained using all channels, and the mean error distance
219 increased as the number of channels decreased (Figure 5). We obtained a mean error distance
220 of less than 1 cm with a number of channels above 17 (Ch_Set4) broadly attached on the motor
221 cortex. In addition, a mean error distance of approximately 1.32 cm was found when using only

222 nine channels attached on the midline of the motor cortex. It was documented that reliable FDI
223 MEP was observed with an area of approximately 12.9 cm^2 ($3.6 \text{ cm} \times 3.6 \text{ cm}$), meaning that
224 a reliable MEP could be evoked with a distance of up to approximately 1.8 cm based on the
225 center of the motor hotspot area [29]. Therefore, although the mean error distance of our
226 proposed motor-hotspot-identification method statistically increased as the number of channels
227 decreased, it is expected that our EEG-based machine-learning approach could be utilized by
228 employing only the motor cortex channels for motor hotspot identification, thereby improving
229 its practicality.

230 The performance of our proposed motor-hotspot-identification method was better when
231 using higher frequency EEG features (delta: $1.20 \pm 0.09 \text{ cm}$; theta: $1.17 \pm 0.10 \text{ cm}$, alpha: 1.05
232 $\pm 0.09 \text{ cm}$, beta: $0.33 \pm 0.03 \text{ cm}$, gamma: $0.22 \pm 0.03 \text{ cm}$, full: $0.30 \pm 0.03 \text{ cm}$). In particular,
233 beta and gamma PSDs showed significantly lower mean error distances than those of delta,
234 theta, and alpha PSDs. Much evidence has been accumulated indicating that a hand motor task
235 significantly changes EEG frequency information in relatively higher frequency bands, i.e.,
236 alpha, beta, and gamma bands [30–34], and thus the higher performance obtained using higher
237 frequency EEG features can be explained from a neurophysiological point of view. However,
238 alpha PSDs did not show better performance as compared to delta and theta PSDs even though
239 alpha band is also closely associated with motor tasks, which should be further investigated in
240 future studies to optimize EEG frequency bands for more accurate motor hotspot identification
241 based on the proposed EEG-based machine-learning approach.

242 The difference between the mean error distances for the left and right hands were not
243 statistically significant for most comparison cases; two cases showed significant difference
244 (full band and Ch_Set3). This might indicate that our proposed approach is not sensitive to
245 handedness for motor hotspot identification. However, as all subjects recruited in this study

246 were right-handed, additional experiments are required with left-handed subjects to carefully
247 address the mentioned hypothesis.

248 The application of tES is not only limited to motor rehabilitation but can also be applied to
249 various psychiatric disorders, such as depression, schizophrenia, and attention deficit
250 hyperactivity disorder, to improve not only their cognitive functions, but also neurologically
251 relieve their symptoms [35–39]. In order to apply tES to psychiatric disorders, a target location
252 should be first determined, similarly to motor hotspots for motor rehabilitation. For cognitive
253 rehabilitation, in general, the anodal electrode is attached to F3 according to the international
254 10-20 system to stimulate the dorsolateral prefrontal cortex (DLPFC), which is known to be
255 associated with various cognitive functions, and the cathodal electrode is attached to F4 or the
256 supraorbital area of the contralateral hemisphere [39–41]. However, as the location of motor
257 hotspots varies from an individual to another, it could be assumed that the tES target location
258 for cognitive rehabilitation is also slightly different between individuals. Therefore, our
259 proposed motor-hotspot-identification approach might be also used for precisely finding a tES
260 target location to maximize the positive effect of cognitive rehabilitation.

261 On the other hand, the proposed motor-hotspot-identification method used the motor hotspot
262 coordinates identified by TMS as an input to construct the ANN model. Considering the
263 practical use of our proposed method without TMS, the motor hotspot information obtained
264 using TMS should be excluded in the process of finding a motor hotspot using a machine
265 learning technique, and thus we will continuously advance our proposed algorithm in such a
266 way that the motor-hotspot-identification algorithm ultimately does not require the motor
267 hotspot information obtained using TMS for a new subject. Despite the mentioned limitation,
268 it is thought that the results shown in this study could prove the proof-of-concept of the
269 proposed EEG-based motor-hotspot-identification method.

270 **Conclusion**

271 In this study, we proposed a novel EEG-based motor-hotspot-identification approach as an
272 alternative to TMS and demonstrated its feasibility via EEG experiments. We also confirmed
273 the possibility of using our proposed method to the development of a practical EEG-based
274 motor-hotspot-identification system with a small number of channels attached only on the
275 motor cortex. Because the brain activity patterns of patients with motor impairment would be
276 different from those of healthy subjects, our proposed motor-hotspot-identification method
277 should be further verified with patients to carefully demonstrate its clinical feasibility.

278

279 **Abbreviations**

280 tES: transcranial electrical stimulation; NIBS: non-invasive brain stimulation; tDCS:
281 transcranial direct current stimulation; tACS: transcranial alternating current stimulation; tRNS:
282 transcranial random noise stimulation; TMS: transcranial magnetic stimulation; ADHD:
283 attention deficit hyperactivity disorder; DLPFC: dorsolateral prefrontal cortex; MEP: motor
284 evoked potential; EEG: electroencephalography; IRB: institutional review board; FDI: first
285 dorsal interosseous; EMG: electromyography; ICA: independent component analysis; PSD:
286 power spectral density; FFT: fast Fourier transform; ANN: artificial neural network; MRCP:
287 movement-related cortical potential.

288

289 **Acknowledgements**

290 Not applicable.

291

292 **Authors' contributions**

293 GYC, NJP, WSK, and HJH participated in designing the experimental paradigm, interpreted

294 the data, and drafted the manuscript. GYC and HTL conducted data collection, and GYC and
295 CHH analyzed the data.

296 **Funding**

297 This work was supported by Ministry of Trade Industry & Energy (MOTIE, Korea), Ministry
298 of Science & ICT (MSIT, Korea), and Ministry of Health & Welfare (MOHW, Korea) under
299 Technology Development Program for AI-Bio-Robot-Medicine Convergence (20001650), and
300 by Basic Science Research Program through the National Research Foundation of Korea (NRF)
301 funded by the Ministry of Education (No. 2019R111A3A01060732).

302 **Availability of data and material**

303 All data measured and analyzed during this study will be published in a public repository after
304 official publication.

305

306 **Competing interests**

307 The authors declare no competing interests.

308

309 **Ethics approval and consent to participate**

310 This study was approved by the Institutional Review Board (IRB) of Kumoh National Institute
311 of Technology (No. 6250) and was conducted in accordance with the principles of the
312 declaration of Helsinki.

313

314 **Consent for publication**

315 cNot applicable. No subject is identifiable by the data presented in the figures and tables.

316

317 Reference

318

319 1. Hummel FC, Cohen LG: **Non-invasive brain stimulation: a new strategy to improve**
320 **neurorehabilitation after stroke?** *Lancet Neurol* 2006, **5**: 708-712.

321 2. Lang AE, Lozano AM: **Parkinson's disease.** *N Engl J Med* 1998, **339**: 1130-1143.

322 3. Rowland LP, Shneider NA: **Amyotrophic lateral sclerosis.** *N Engl J Med* 2001, **344**:
323 1688-1700.

324 4. Jeffery DT, Norton JA, Roy FD, Gorassini MA: **Effects of transcranial direct current**
325 **stimulation on the excitability of the leg motor cortex.** *Exp Brain Res* 2007, **182**: 281-
326 287.

327 5. Dmochowski JP, Datta A, Huang Y, Richardson JD, Bikson M, Fridriksson J, Parra LC:
328 **Targeted transcranial direct current stimulation for rehabilitation after**
329 **stroke.** *Neuroimage* 2013, **75**: 12-19.

330 6. Claflin ES, Krishnan C, Khot SP: **Emerging treatments for motor rehabilitation after**
331 **stroke.** *Neurohospitalist* 2015, **5**: 77-88.

332 7. Klomjai W, Lackmy-Vallée A, Roche N, Pradat-Diehl P, Marchand-Pauvert V, Katz R:
333 **Repetitive transcranial magnetic stimulation and transcranial direct current**
334 **stimulation in motor rehabilitation after stroke: an update.** *Ann Phys Rehab Med* 2015,
335 **58**: 220-224.

336 8. Koh CL, Lin JH, Jeng JS, Huang SL, Hsieh CL: **Effects of Transcranial direct current**
337 **stimulation with sensory modulation on stroke motor rehabilitation: a randomized**
338 **controlled trial.** *Arch Phys Med Rehab* 2017, **98**: 2477-2484.

339 9. Nitsche MA, Paulus W: **Excitability changes induced in the human motor cortex by**
340 **weak transcranial direct current stimulation.** *J Physiol* 2000, **527**: 633-639.

341 10. Antal A, Boros K, Poreisz C, Chaieb L, Terney D, Paulus W: **Comparatively weak after-**
342 **effects of transcranial alternating current stimulation (tACS) on cortical excitability**
343 **in humans.** *Brain Stimul* 2008, **1**: 97-105.

344 11. Allman C, Amadi U, Winkler AM, Wilkins L, Filippini N, Kischka U, Johansen-Berg H:
345 **Ipsilesional anodal tDCS enhances the functional benefits of rehabilitation in patients**
346 **after stroke.** *Sci Transl Med* 2016, **8**: 330re1-330re1.

347 12. Del Felice A, Castiglia L, Formaggio E, Cattelan M, Scarpa B, Manganotti P, Masiero S:
348 **Personalized transcranial alternating current stimulation (tACS) and physical**
349 **therapy to treat motor and cognitive symptoms in Parkinson's disease: A randomized**

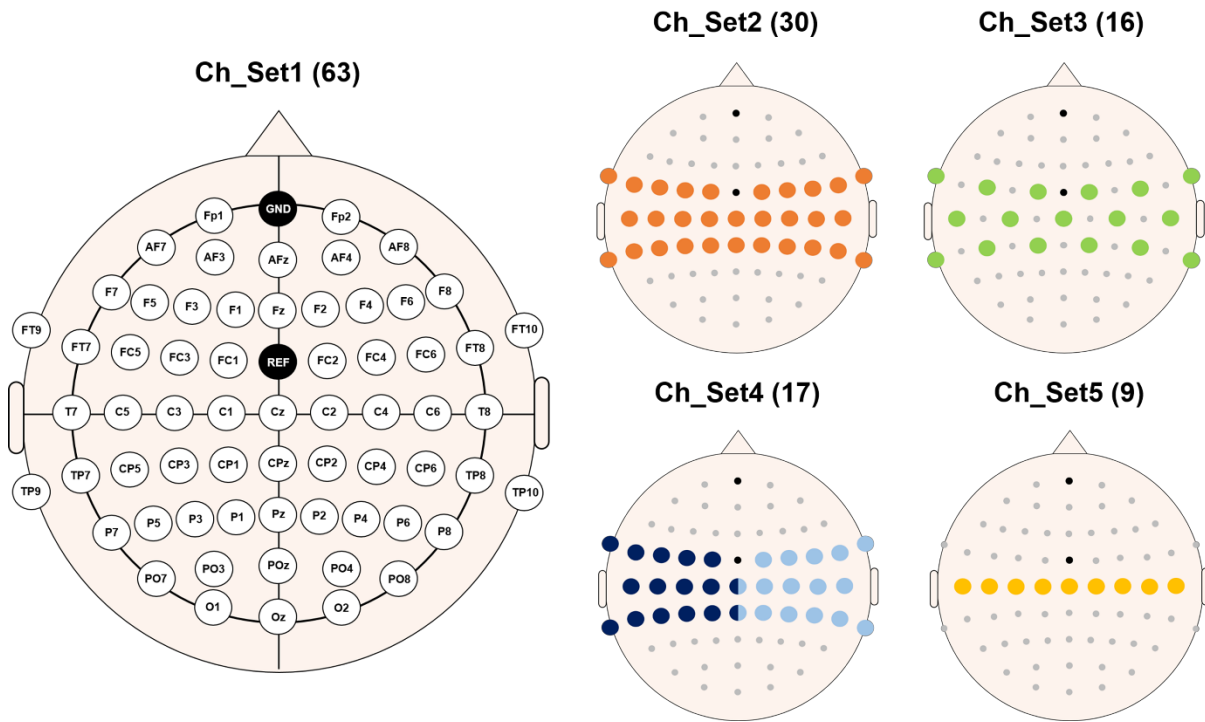
- 350 **cross-over trial.** *NeuroImage Clin* 2019, **22**: 101768.
- 351 13. Bolognini N, Vallar G, Casati C, Latif LA, El-Nazer R, Williams J, Fregni F:
352 **Neurophysiological and behavioral effects of tDCS combined with constraint-induced**
353 **movement therapy in poststroke patients.** *Neurorehab Neural Re* 2011, **25**: 819-829.
- 354 14. Waters-Metenier S, Husain M, Wiestler T, Diedrichsen J: **Bihemispheric transcranial**
355 **direct current stimulation enhances effector-independent representations of motor**
356 **synergy and sequence learning.** *J Neurosci* 2014, **34**: 1037-1050.
- 357 15. Ferreira IS, Costa BT, Ramos CL, Lucena P, Thibaut A, Fregni F: **Searching for the**
358 **optimal tDCS target for motor rehabilitation.** *J NeuroEng Rehab* 2019, **16**: 90.
- 359 16. Boggio PS, Castro LO, Savagim EA, Braitte R, Cruz VC, Rocha RR, Fregni F:
360 **Enhancement of non-dominant hand motor function by anodal transcranial direct**
361 **current stimulation.** *Neuroscience* 2006, **404**: 232-236.
- 362 17. Wade S, Hammond G: **Anodal transcranial direct current stimulation over premotor**
363 **cortex facilitates observational learning of a motor sequence.** *Eur J Neuroscience* 2015,
364 **41**: 1597-1602.
- 365 18. Ferrucci R, Vergari M, Cogiamanian F, Bocci T, Ciocca M, Tomasini E, de Riz M, Scarpini
366 E, Priori A: **Transcranial direct current stimulation (tDCS) for fatigue in multiple**
367 **sclerosis.** *NeuroRehabilitation* 2014, **34**: 121-127.
- 368 19. Volpe JJ: **Brain injury in the premature infant—from pathogenesis to prevention.** *Brain*
369 *Dev* 1997, **19**: 519-534.
- 370 20. Yousry TA, Schmid UD, Alkadhi H, Schmidt D, Peraud A, Buettner A, Winkler P:
371 **Localization of the motor hand area to a knob on the precentral gyrus. A new**
372 **landmark.** *Brain* 1997, **120**: 141-157.
- 373 21. Boroojerdi B, Foltys H, Krings T, Spetzger U, Thron A, Töpper R: **Localization of the**
374 **motor hand area using transcranial magnetic stimulation and functional magnetic**
375 **resonance imaging.** *Clin Neurophysiol* 1999, **110**: 699-704.
- 376 22. Weise K, Numssen O, Thielscher A, Hartwigsen G, Knösche TR: **A novel approach to**
377 **localize cortical TMS effects.** *NeuroImage* 2020, 209:116486.
- 378 23. Choi GY, Han CH, Lim H, Lim, Ku J, Kim WS, Hwang HJ: **Electroencephalography-**
379 **based Motor Hotspot Detection.** *In Procs of the 13th International Joint Conference on*
380 *Biomedical Engineering Systems and Technologies* 2020, **4**: 195-198.
- 381 24. Szubski C, Burtscher M, Loscher WN: **The effects of short-term hypoxia on motor**
382 **cortex excitability and neuromuscular activation.** *J Appl Physiol* 2006, **101**: 1673-1677.

- 383 25. Wiethoff S, Hamada M, Rothwell JC: **Variability in response to transcranial direct**
384 **current stimulation of the motor cortex.** *Brain Stimul* 2014, **7**: 468-475.
- 385 26. Hannah R, Iacovou A, Rothwell JC: **Direction of TDCS current flow in human**
386 **sensorimotor cortex influences behavioural learning.** *Brain Stimul* 2019, **12**: 684-692.
- 387 27. Shibasaki H, Hallett M: **What is the Bereitschaftspotential?** *Clin Neurophysiol* 2006, **117**:
388 2341-2356. <https://doi.org/10.1016/j.clinph.2006.04.025>.
- 389 28. Jochumsen M, Niazi IK, Mrachacz-Kersting N, Farina D, Dremstrup K: **Detection and**
390 **classification of movement-related cortical potentials associated with task force and**
391 **speed.** *J Neural Eng* 2013, **10**: 056015. doi: 10.1088/1741-2560/10/5/056015.
- 392 29. Malcolm MP, Triggs WJ, Light KE, Shechtman O, Khandekar G, Rothi LG: **Reliability of**
393 **motor cortex transcranial magnetic stimulation in four muscle representations.** *Clin*
394 *Neurophysiol* 2006, **117**: 1037-1046. <https://doi.org/10.1016/j.clinph.2006.02.005>.
- 395 30. Hwang HJ, Kim KH, Jung YJ, Kim DW, Lee YH, Im CH: **An EEG-based real-time**
396 **cortical functional connectivity imaging system.** *Med Biol Eng Comput* 2011, **49**: 985-
397 995.
- 398 31. Lee NG, Kang SK, Lee DR, Hwang HJ, Jung JH, You JSH, Im CH, Kim DA, Jung A, Lee
399 PT, Ki S, Kim KS: **Feasibility and test-retest reliability of an electroencephalography-**
400 **based brain mapping system in children with cerebral palsy: a preliminary**
401 **investigation.** *Arch Phys Med Rehab* 2012, **93**: 882-888.
- 402 32. Murta T, Chaudhary UJ, Tierney TM, Dias A, Leite M, Carmichael DW, Carmichael P,
403 Lemieux L: **Phase–amplitude coupling and the BOLD signal: a simultaneous**
404 **intracranial EEG (icEEG)-fMRI study in humans performing a finger-tapping**
405 **task.** *Neuroimage* 2017, **146**: 438-451.
- 406 33. Stavrinou ML, Moraru L, Cimponeriu L, Della Penna S, Bezerianos A: **Evaluation of**
407 **cortical connectivity during real and imagined rhythmic finger tapping.** *Brain*
408 *Topogr* 2007, **19**: 137-145.
- 409 34. Ginter JrJ, Blinowska KJ, Kamiński M, Durka PJ, Pfurtscheller G, Neuper C: **Propagation**
410 **of EEG activity in the beta and gamma band during movement imagery in**
411 **humans.** *Method Inform Medicine* 2005, **44**: 106-113.
- 412 35. Dallmer-Zerbe I, Popp F, Lam AP, Philipsen A, Herrmann CS: **Transcranial Alternating**
413 **Current Stimulation (tACS) as a Tool to Modulate P300 Amplitude in Attention**
414 **Deficit Hyperactivity Disorder (ADHD): Preliminary Findings.** *Brain Topogr* 2020, **33**:
415 191-207.

- 416 36. Breitling C, Zaehle T, Dannhauer M, Bonath B, Tegelbeckers J, Flechtner HH, Krauel K:
417 **Improving interference control in ADHD patients with transcranial direct current**
418 **stimulation (tDCS).** *Front Cell Neurosci* 2016, **10**: 72.
- 419 37. Brunelin J, Mondino M, Gassab L, Haesebaert F, Gaha L, Suaud-Chagny MF, Poulet E, et
420 al: **Examining transcranial direct-current stimulation (tDCS) as a treatment for**
421 **hallucinations in schizophrenia.** *Am J Psychiatry* 2012, **169**: 719-724.
- 422 38. George MS, Nahas Z, Molloy M, Speer AM, Oliver NC, Li XB, Ballenger JC, et al: **A**
423 **controlled trial of daily left prefrontal cortex TMS for treating depression.** *Biol*
424 *Psychiatry* 2000, **48**: 962-970.
- 425 39. Nitsche MA, Boggio PS, Fregni F, Pascual-Leone A: **Treatment of depression with**
426 **transcranial direct current stimulation (tDCS): a review.** *Exp Neurol* 2009, **219**: 14-19.
- 427 40. Fregni F, Boggio PS, Nitsche MA, Rigonatti SP, Pascual-Leone A: **Cognitive effects of**
428 **repeated sessions of transcranial direct current stimulation in patients with**
429 **depression.** *Depress Anxiety* 2006, **23**: 482-484.
- 430 41. Padberg F, Kumpf U, Mansmann U, Palm U, Plewnia C, Langguth B, Keeser D, et al:
431 **Prefrontal transcranial direct current stimulation (tDCS) as treatment for major**
432 **depression: study design and methodology of a multicenter triple blind randomized**
433 **placebo controlled trial (DepressionDC).** *Eur Arch Psy Clin N* 2017, **267**: 751-766.
434
435
436

437 **Figure Captions**

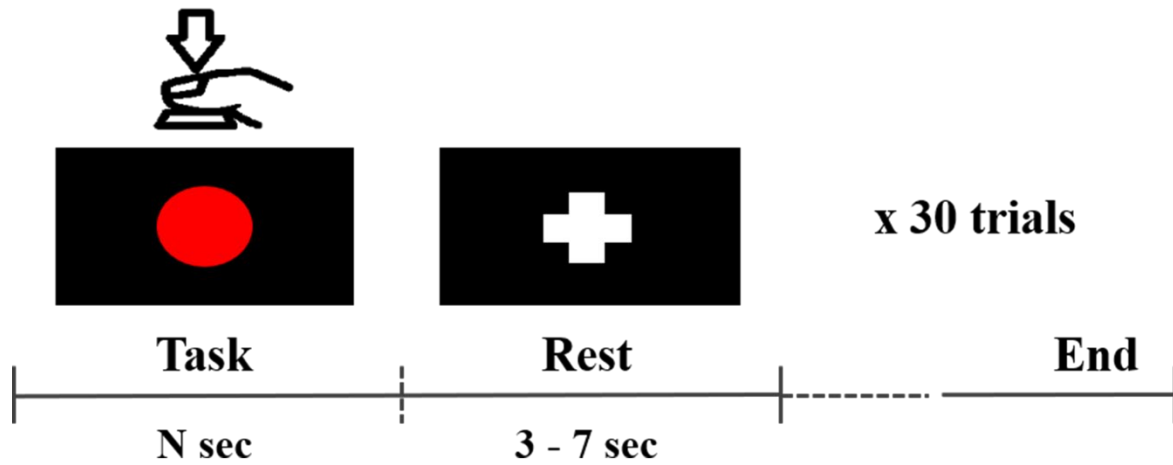
438



439

440

441 Figure 1. Electrode sites used for EEG data measurement. Five different channel sets were used
442 for data analysis in order to study the impact of the number of channels on the error distance
443 of motor hotspot location. Channels denoted by different colors in Ch_Set4 represent those
444 selected on the contralateral motor cortex for the data analysis of each hand. The numbers in
445 parentheses indicate the numbers of channels for the corresponding channel set.

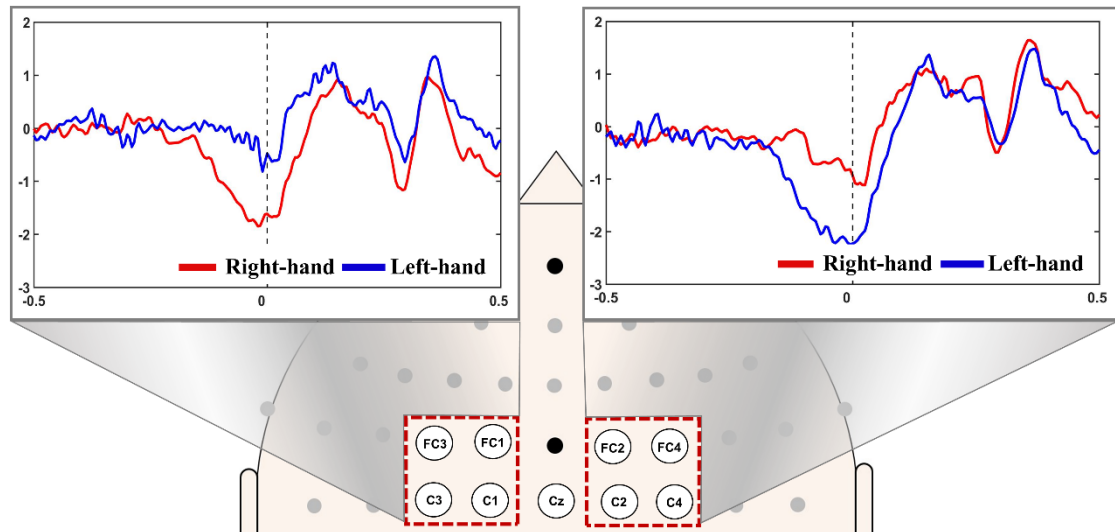


446

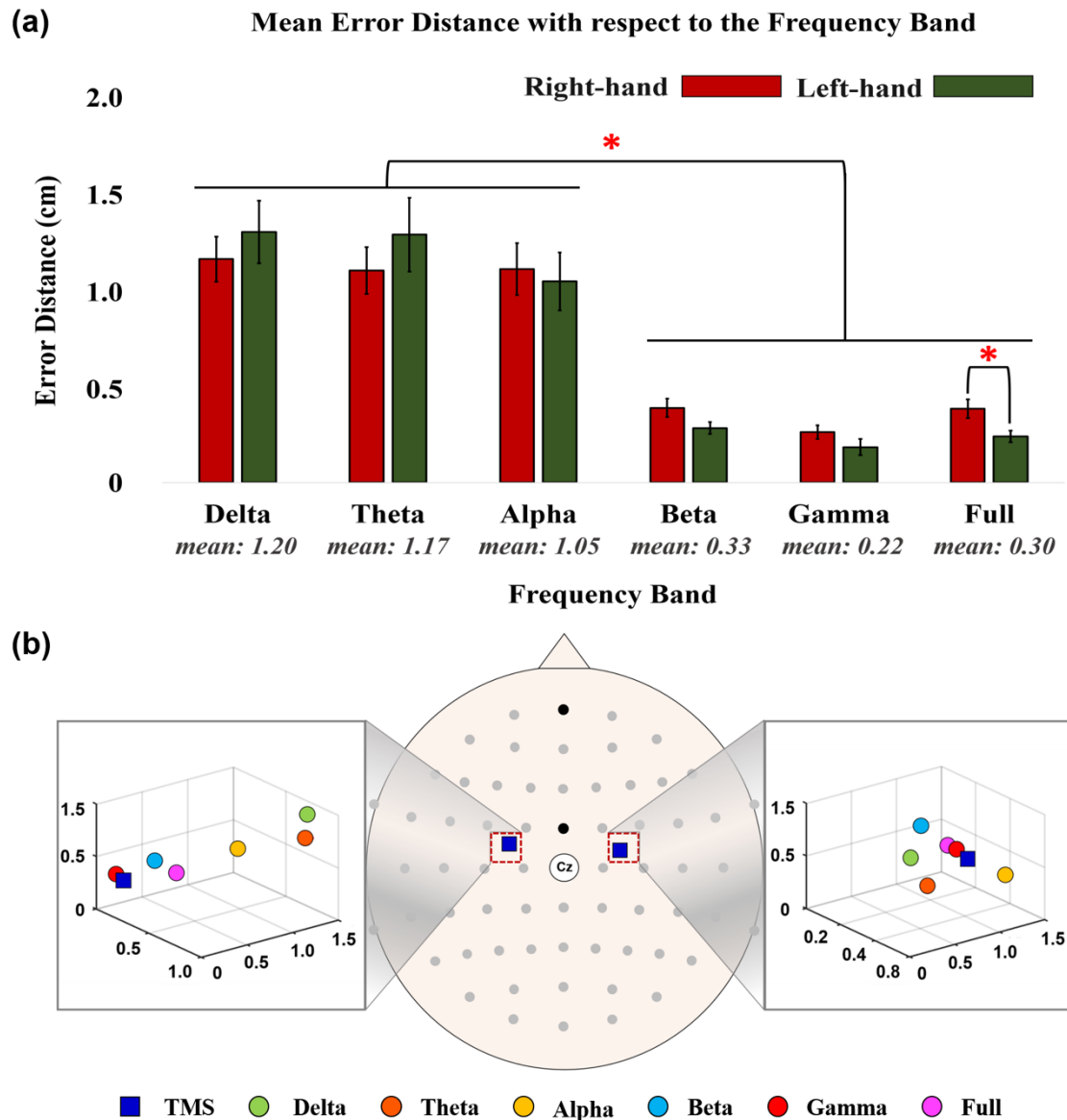
447

448 Figure 2. Experimental paradigm used in this study. Each subject presses a space bar whenever
449 the red circle is presented in the middle of a screen. The red circle is maintained until the subject
450 presses the space bar. After the task period, the fixation ('+') mark is presented to indicate a
451 rest period.

452



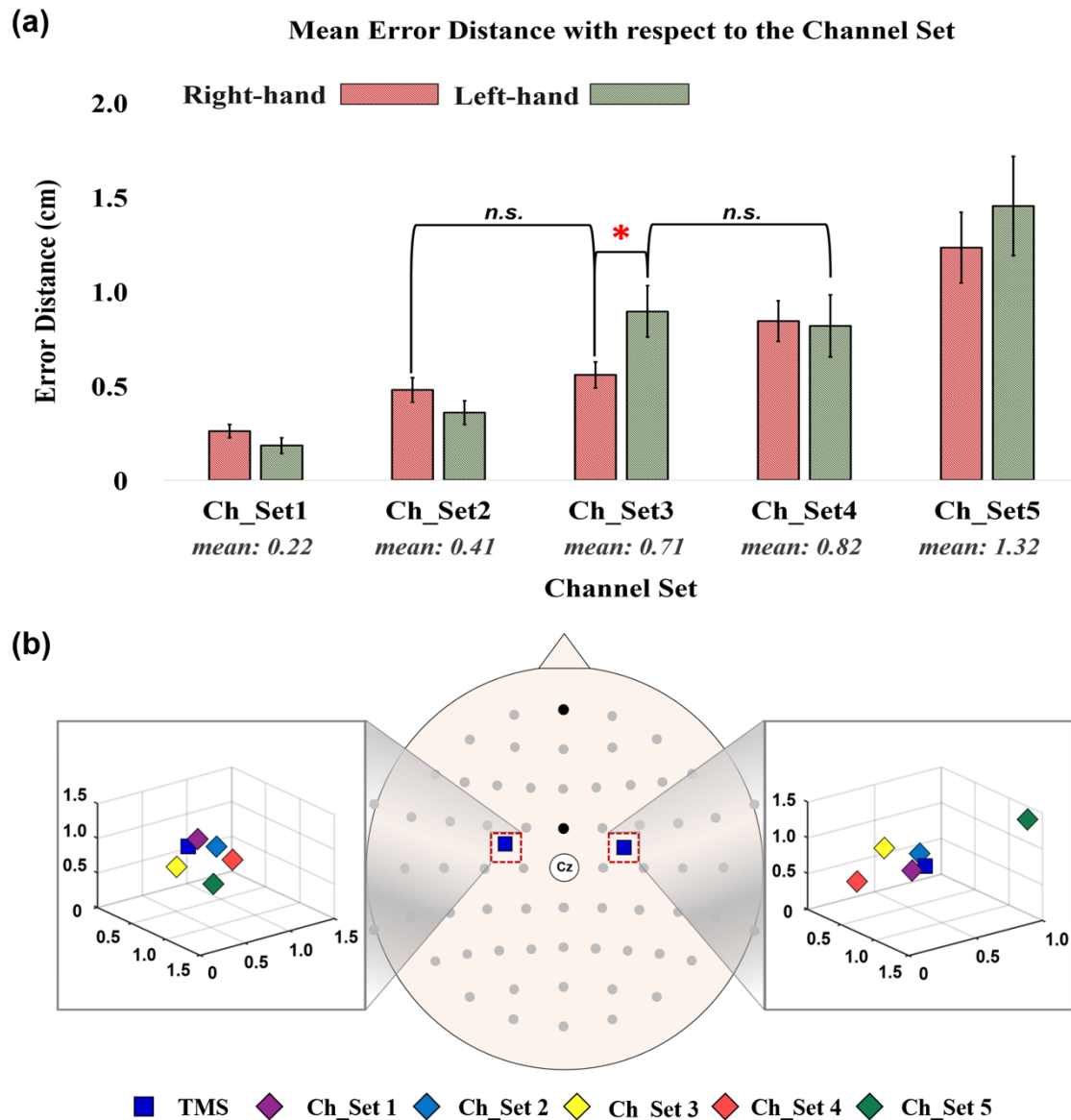
453
454 Figure 3. Grand averaged movement-related cortical potential (MRCP) patterns of all subjects
455 on both hemispheres. Contralateral MRCPs are clearly observed.
456



457

458

459 Figure 4. (a) Mean error distances between the motor hotspot locations identified by TMS-
 460 induced MEP and our EEG-based machine learning approach with respect to the frequency
 461 band (RM-ANOVA with Bonferroni corrected p -value < 0.05 : delta = theta = alpha $>$ beta =
 462 gamma = full for both hands). The numbers below the bar graphs represent the mean error
 463 distances of the left and right hands. No significant difference was observed between the left
 464 and right hands for all the frequency bands in terms of the error distance (paired t -test $p > 0.05$),
 465 except the full band (right hand $>$ left hand). (b) A representative example showing the 3D
 466 locations of the motor hotspots identified by TMS-induced MEP (blue rectangle) and our EEG-
 467 based approach with respect to the frequency band.



468
 469 Figure 5. (a) Mean error distances between the motor hotspot locations identified by TMS-
 470 induced MEP and our EEG-based machine learning approach with respect to the number of
 471 channels (RM-ANOVA with Bonferroni corrected p -value < 0.05: Ch_Set5 > Ch_Set4 >
 472 Ch_Set3 = Ch_Set2 > Ch_Set1 for the right hand and Ch_Set5 > Ch_Set4 = Ch_Set3 > Ch_Set2
 473 > Ch_Set1 for the left hand). The numbers below the bar graphs represent the mean error
 474 distances of the left and right hands. No significant difference was observed between the left
 475 and right hand for all channel sets in terms of the error distance (paired t-test $p > 0.05$), except
 476 Ch_Set3 (left hand > right hand). The abbreviation, *n.s.*, means no significant difference. (b) A
 477 representative example showing the 3D locations of the motor hotspots identified by TMS (blue
 478 rectangle) and the EEG-based approach with respect to the number of channels.